ISSN 1392–1207. MECHANIKA. 2017 Volume 23(2): 168–175

Statistical evolution of short fatigue crack growth rate for LZ50 axle steel

B. Yang*, Z. Liao, B.Q. Ma***, Y.Y. Wu****, S.N. Xiao*****

**State Key Laboratory of Traction Power, Southwest Jiaotong University, 610031, Chengdu, China, E-mail: yb@swjtu.cn*
***State Key Laboratory of Traction Power, Southwest Jiaotong University, 610031, Chengdu, China, E-mail: 1442868474@qq.com*
****State Key Laboratory of Traction Power, Southwest Jiaotong University, 610031, Chengdu, China, E-mail: 1169034492@qq.com*
*****State Key Laboratory of Traction Power, Southwest Jiaotong University, 610031, Chengdu, China, E-mail: 407777376@qq.com*
******State Key Laboratory of Traction Power, Southwest Jiaotong University, 610031, Chengdu, China, E-mail: snxiao@swjtu.cn*

crossref http://dx.doi.org/10.5755/j01.mech.23.2.18108

1. Introduction

Fatigue fracture is the main failure mode of most mechanical components [1]. Meanwhile, the initiation and propagation of fatigue crack for smooth surface components occupy the most part of service life [2]. The behavior of short fatigue crack, which is strongly affected by microstructure in the microstructure short crack (MSC) stage and large scale yielding in the physical short crack (PSC) stage, is not similar with conventional long crack [3-5]. Therefore, method of linear elastic fracture mechanics (LEFM) cannot be applied to solving short crack problems directly while the research of short fatigue crack behavior is of great importance.

The behavior of short fatigue cracks, which is strongly affected by microstructure in the MSC stage and by merge propagation mechanism in the PSC stage, shows a large scatter and obvious statistical characteristics. Therefore the probabilistic method should be one of the feasible analytical approaches for describing short fatigue crack behaviour [2, 6, 7]. During the past three decades, by using 3-parameter Weibull distribution (3PWD), 2-parameter Weibull distribution (2PWD) and considering the fitting effect, Goto [8-10], Suh [11] and Akiniwa [12] analyzed four typical characteristic parameters of short fatigue crack, i.e., the dominant effective short fatigue crack (DESFC) sizes, the fatigue life fraction, the effective short fatigue cracks (ESFCs) density, and the DESFC growth rates. Conclusions were drawn that all data scattered largely in the MSC stage and had a trend to be consistent in the PSC stage. However, these conclusions were based on the unilateral considerations of fitting effect, while consistency with the relevant fatigue physics and safety of design evaluation were not taken into account.

In engineering applications, to achieve the reasonable damage tolerance design and safety assessment in-service, penetrating understanding of characteristic of statistics evolution of short fatigue crack is necessary [2]. Above four typical characteristic parameters were analyzed using seven distributions on three aspects, i.e., total fitting effect, consistency with the relevant fatigue physics and safety of design evaluation, by Zhao [2, 7, 13, 14] and the authors [15]. It is considered that normal distribution (ND), extreme minimum distribution (EMVD1), extreme maximum distribution (EMVD2), and lognormal distribution (LND) were the good distributions for these typical parameters of short crack behavior, instead of 3PWD and 2PWD.

LZ50 axle steel is one of the important materials widely used in the manufacture of axle for the speed-up and heavy freight rolling stocks in China. The study of its short fatigue crack behavior has important engineering significance [15]. Based on the DESFC sizes corresponding to loading cycles, growth rates of DESFC associated with DESFC size and fatigue life fraction were calculated. On this basis, good distribution for the description of DESFC growth rate data was determined considering three aspects mentioned above.

2. Experimental work

2.1. Material and specimens

Test material of present work is LZ50 axle steel, which is originated from a RE2B type axle. Test specimens were machined into smooth axial hourglass shape, while the axial of specimens were consistent with the axial of the RE2B axle. The minimum diameter of the specimen was 8mm while the arc segment of the specimen was polished to a mirror effect as shown in Fig. 1. The chemical composition of LZ50 axle steel is C 0.47, Si 0.26, Mn 0.78, Cr 0.02, Ni 0.028, Cu 0.15, Al 0.021, P < 0.014, S < 0.007, and the reminder Fe by wt%. Heat treatment conditions are as follows: normalizing heat for 2 hours under 860°C and 800°C, tempering for 1.5 h under 570°C. The tensile tests were carried out on CMT 5105 electronic universal testing machine according to Chinese standard of GB/T 228.1-2010 Metallic materials – Tensile testing – Part 1: Method of test at room temperature. The strain rate was controlled to be 1.0×10^{-3} s^{-1}. Test results at room temperature with 10 specimens showed that the tensile strength is 674 MPa, the yield strength is 342 MPa, the elongation is 20.79%, and the reduction of area is 40.38%. Metallographic test of LZ50 steel showed that the material has a typical "ferrite (white) and lamellar pearlite" structure (Fig. 2, b, with a magnification of 1500), and the pearlite has obvious banded structure (Fig. 2, a, with a magnification of 200) due to the forging process in the manufacture of axle.

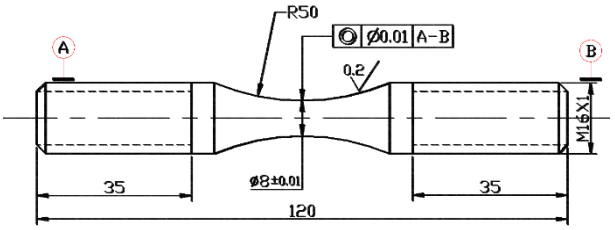

Fig. 1 Schematic of shape and dimension of the specimen for fatigue test (unit: mm)

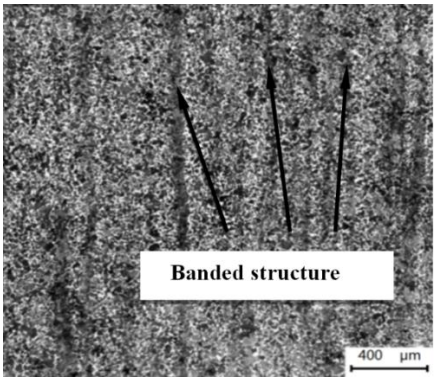

a

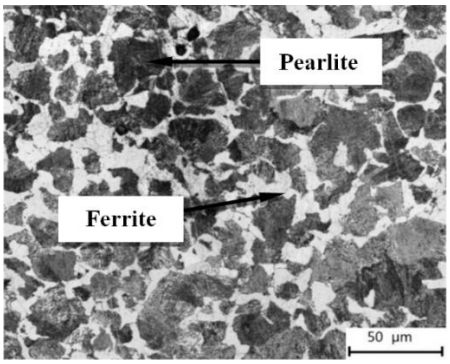

b

Fig. 2 Metallographic test photograph of LZ50 axle steel: a - with a magnification of 200; b - with a magnification of 1500

Before fatigue test, the central arc surface of the specimen was etched with 4% nitric acid alcohol solution so as to expose the metallographic structures. It has been showed that the short crack behavior was not affected by this kind of surface treatment method, because the etching depth is smaller than the roughness of finest engineering surface [2]. All replica tests were conducted on MTS 809 type axial tension and torsion fatigue testing machine following ASTM E647-11 Standard Test Method for Measurement of Fatigue Crack Growth Rates. The tests were performed under sine loading wave with a loading frequency of 15 Hz. The stress amplitude was controlled to be 225 MPa and the stress ratio was 0.1. In the loading process, the test was interrupted at predetermined cycle number. Then, cellulose acetate film soften by acetone was pasted on the specimen arc surface. Once the film was dry, it was peeled off and saved by two glass slides. Above step was repeated until the specimen was fractured finally. The more times the surface of specimen was replicated, the more comprehensive the short fatigue crack behavior could be. Therefore, the given cyclic interval should be as small as possible to ensure that the number of effective replicating times for each specimen was no less than 10 times. At the same time, to make the crack be in an open state during surface replicating process, a tensile stress of 10 MPa was retained when the test machine was stopped temporarily.

2.2. Fatigue test results

The dried replica films were examined step by step according to "the reverse observation method" [16] from failure to fatigue initiation using Olympus OLS4100 3D measuring laser microscope. Ultimately, cracks information, i.e., the crack length, crack angle and number of cracks, of each specimen at every effective replica film were obtained. The "effective short fatigue crack criterion" proposed by Zhao [2, 16] has established the basic frame of the study of short fatigue crack behavior. Based on this criterion, the original data of DESFC scale at each replica were obtained and the DESFC growth rates with corresponding DESFC size or fatigue life fraction were calculated and given in Fig. 3.

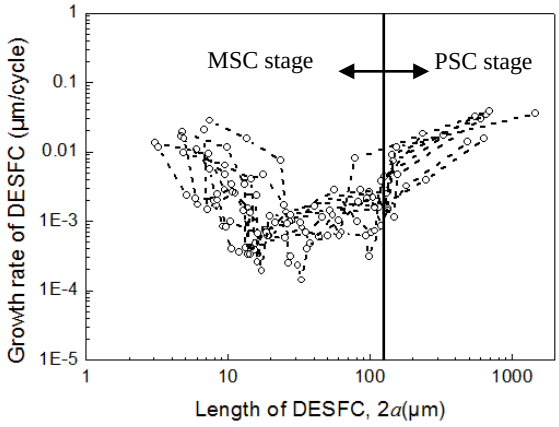

a

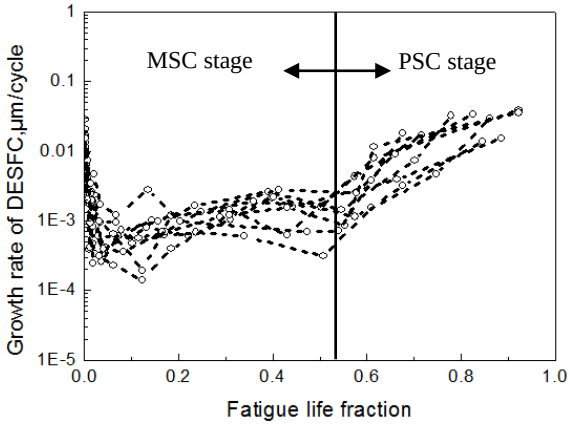

b

Fig. 3 DESFC growth rate of LZ50 axle steel with corresponding DESFC size and fatigue life fraction: a - at given DESFC size; b - at given fatigue life fraction

The figure shows that the DESFC growth rates of all specimens are different to a certain extent, but the growth rate of DESFC decreases twice during the crack propagation process for every specimen. Combined with the work in reference [15], conclusion can be drawn that the reason for two

significant decreases of DESFC growth rate lies in the restrains of ferrite grain boundary and the rich pearlite banded structure. Statistical calculation indicates that when the first decrease of DESFC growth rate occurs, the average DESFC size is 14.18 μm which is close to the ferrite equivalent diameter, while the mean square deviation is 5.18 μm. The mean life fraction is about 0.03448 correspondingly. When the second decrease occurs, the average DESFC size is 113.74 μm on average which is close to the interval of rich pearlite banded structure, while the mean square deviation is 16.61 μm. Corresponding mean life fraction is about 0.54872.

3. Statistical analysis

3.1. Analysis of DESFC growth rate at given characteristic DESFC size

Using linear interpolation method, the DESFC growth rates ($d2a / dN$) of all specimens under 10 given characteristic DESFC sizes ($2a$) were obtained. All DESFC growth rates and its mean value are showed in Fig. 4, which show that the mean value of DESFC growth rate decreases twice with the increase of DESFC size. The corresponding DESFC sizes are 30 μm and 100 μm, which roughly equivalent to the average diameter of ferrite and the interval of rich pearlite banded structure respectively.

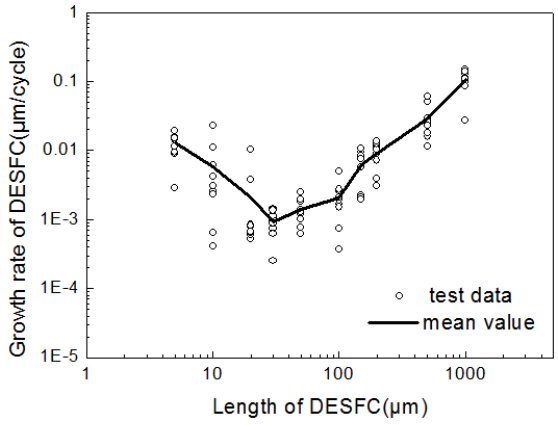

Fig. 4 DESFC growth rate at given DESFC size

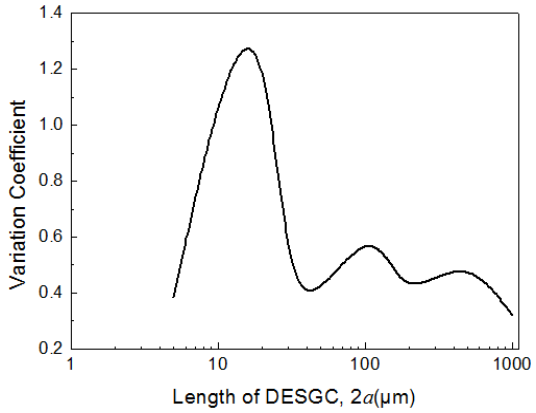

Fig. 5 Variation coefficient of DESFC growth rate at given DESFC size

Average DESFC growth rate $(\mathrm{d}a / \mathrm{d}N)_{m1}$, standard deviations of DESFC growth rate $(\mathrm{d}a / \mathrm{d}N)_{s1}$ and coefficients of variation Cv_1 of all the 9 specimens under 10 given characteristic DESFC size ($2a$) are listed in Table 1. Meanwhile, the evolution of Cv_1 with the DESFC size is given in Fig. 5, which shows that coefficients of variation Cv_1 reached its maximum value when DESFC size, $2a$, is equal to 20 μm. Then Cv_1 gradually declines with fluctuations. This leads to the results that the scatter of the DESFC growth rates data rises in early stage and then fall in later stage. The reason is that the short fatigue cracks are strongly affected by microstructures in the MSC stage. With the establishment of DESFC and the merge of ESFCs in the PSC stage, the influences of microstructures are not that significant any more.

Reference [17] proposed a statistical method by taking the total fitting effect, the consistency with the relevant fatigue physics and the safety of design evaluation into account. This method can determine the good distribution with limited fatigue test data by comparing 7 commonly used distributions including 3PWD, 2PWD, ND, LND, EMVD1, EMVD2 and exponential distribution (ED). The linear correlation coefficients of DESFC growth rate at 10 given characteristic DESFC sizes for the above 7 distributions were given in Table 2. From the view of best fitting effect, namely the extent how the value of $\left|R_{XY}\right|$ is close to 1, the order of best fit is 3PWD, ND, 2PWD, LND, ED, EMVD1 and EMVD2. For the first five distributions, 9 groups of linear correlation coefficients were all greater than 0.85, but for EMVD1 and EMVD2 the values are relatively poor.

Considering the safety of design evaluation, the data of growth rate belongs to the right-tail problem. Reference [18] defines two parameters, i.e., d_{F1} and d_{F2}, to reflect the prediction deviation. For the right-tail problem, d_{F1} and d_{F2} represent the deviation between probability experience and predictive value according to two maximum data, i.e., x_n and x_{n-1}, respectively. At the same time, the reference pointed out: the smaller the $\left|d_F\right|$ is, the smaller the prediction deviation is. Furthermore, if $d_{F1} < d_{F2}$ and $d_{F1} < 0$, when $x > x_n$, the predicted results would tend to be conservative.

The prediction deviation, i.e., d_{F1} and d_{F2}, for 7 commonly used distributions of the right tail failure proportion for the DESFC growth rate data at characteristic DESFC size were given in Table 3. With the consideration of total fitting effect, conclusions can be drawn that ND is the best distribution for DESFC growth rates under DESFC scale. Among the 10 groups of growth rate data in Table 3, the prediction deviations for 7 groups of data show that $d_{F1} < 0$ and $d_{F1} < d_{F2}$ for 7 groups of data. Which means that the predicted values will be relatively conservative as long as the expansion rate is greater than a value of $(d2a / dN)_n$. At the same time, the ND conforms to the consistency with the relevant fatigue physics of the increase of failure ratio with the increase of the growth rate [18]. In conclusion, ND is the best distribution to describe the DESFC growth rates data. Table 4 indicated the cumulative distribution parameters of ND for the DESFC growth rate data showed in Table 3. Corresponding cumulative distribution curve of DESFC growth rate of each group were given in Fig. 6.

Table 1

Statistical parameters of DESFC growth rate at given DESFC size

$2a$, μm	$(da / dN)_{m1}$, $\times 10^{-6}$ m/cycle	$(da / dN)_{s1}$, $\times 10^{-6}$ m/cycle	Cv_1
5	0.0129	0.0049	0.3838
10	0.0059	0.0067	1.1320
20	0.0021	0.0030	1.4493
30	0.0009	0.0004	0.3736
50	0.0014	0.0006	0.4011
100	0.0021	0.0013	0.6145
150	0.0062	0.0032	0.5115
200	0.0091	0.0035	0.3870
500	0.0288	0.0154	0.5352
1000	0.1064	0.0339	0.3191

Table 2

Linear correlation coefficients of DESFC growth rate at 10 given characteristic DESFC sizes for 7 commonly used distributions

$2a_i$, μm	R_{XY}						
	3PWD	2PWD	ND	LND	EMVD1	EMVD2	ED
5	0.939	0.939	0.97	0.8839	0.9865	-0.9295	-0.865
10	0.9849	0.9796	0.8596	0.9853	0.7785	-0.9261	-0.9688
20	0.9428	0.7549	0.728	0.8366	0.6306	-0.8188	-0.8877
30	0.9623	0.9623	0.9884	0.9161	0.9945	-0.9592	-0.9051
50	0.9943	0.9885	0.9823	0.9922	0.9465	-0.9937	-0.9801
100	0.9791	0.9791	0.9416	0.9571	0.8987	-0.9681	-0.9684
150	0.9286	0.9286	0.9546	0.9161	0.9434	-0.9354	-0.8929
200	0.9615	0.9615	0.9678	0.9221	0.981	-0.9276	-0.8631
500	0.9840	0.9563	0.9242	0.9794	0.8658	-0.962	-0.9760
1000	0.8940	0.8940	0.9405	0.8314	0.9692	-0.8952	-0.8254

Table 3

Prediction deviation for 7 commonly used distributions of the right tail failure proportion for the DESFC growth rate data at given characteristic DESFC size

DESFC	$2a_i$, μm	5	10	20	30	50	100	150	200	500	1000
3PWD	d_{F1}	0.0246	-0.0045	0.0011	0.0238	-0.0034	0.0062	-0.0578	-0.0064	0.0037	0.0256
	d_{F2}	-0.1404	0.0329	-0.1332	-0.0932	0.0227	0.011	0.0321	0.0588	-0.0445	-0.1926
2PWD	d_{F1}	0.0246	-0.024	-0.1962	0.0238	-0.0215	0.0062	-0.0578	-0.0064	-0.0390	0.0256
	d_{F2}	-0.1404	0.0384	-0.1212	-0.0932	0.0248	0.011	0.0321	0.0588	-0.0287	-0.1926
ND	d_{F1}	0.0286	-0.1979	-0.2985	0.0259	-0.049	-0.0656	-0.0616	-0.0039	-0.1104	0.0443
	d_{F2}	-0.0755	-0.1003	-0.1991	0.0425	0.0066	-0.0168	0.0346	0.0734	-0.0724	0.1352
LND	d_{F1}	0.0457	0.0004	-0.2071	0.0463	0.003	0.0311	-0.0478	0.0128	-0.0147	0.0453
	d_{F2}	-0.189	0.0496	-0.1422	-0.133	0.0308	0.0058	0.0365	0.0656	-0.0362	-0.2459
EMVD1	d_{F1}	0.0031	-0.1888	-0.2705	-0.0008	-0.0677	-0.0819	-0.0726	-0.0243	-0.1184	0.0194
	d_{F2}	-0.0519	-0.089	-0.1695	-0.0283	0.0009	-0.0182	0.0262	0.0597	-0.0628	-0.0978
EMVD2	d_{F1}	0.0601	-0.1939	-0.3214	0.0596	-0.01	-0.0263	-0.0362	0.0293	-0.0826	0.0691
	d_{F2}	-0.0984	-0.0997	-0.2242	-0.0513	0.029	0.0022	0.0566	0.1007	-0.071	-0.1742
ED	d_{F1}	-0.2446	0.0299	-0.0357	-0.3193	-0.4953	-0.1194	-0.2693	-0.3672	-0.3503	-0.3255
	d_{F2}	-0.5213	0.1112	0.0531	-0.5296	-0.4661	-0.1672	-0.1875	-0.3343	-0.3579	-0.6203

Table 4

Cumulative distribution parameters of ND for the DESFC growth rate data at given characteristic DESFC size

2a, μm	Position parameter μ	Scale parameter σ
5	0.0129	0.006
10	0.0059	0.0091
20	0.0021	0.0049
30	0.0009	0.0004
50	0.0014	0.0007
100	0.0021	0.0016
150	0.0062	0.0039
200	0.0091	0.0043
500	0.0288	0.0195
1000	0.1064	0.0421

By synthesizing Table 1 to Table 3 and Fig. 4 to Fig. 6, conclusions can be drawn as follows:

1. The mean curve of DESFC growth rate decreases twice with the increase of DESFC size. The characteristic sizes when these two growth rate decreases occur are 20 μm and 100 μm, respectively. The standard deviations reach the minimum value when the DESFC size is 30 μm.

2. The scatter of DESFC growth rates data at given characteristic DESFC sizes is large, and with the propagation of cracks, the scatter continues to fluctuate and decline. It is worth noting that, as the DESFC size 2a is equal to 5 μm, the scatter of the DESFC growth rate data is smaller.

3. ND is the best statistical distribution to describe the DESFC growth rates data at given characteristic DESFC sizes.

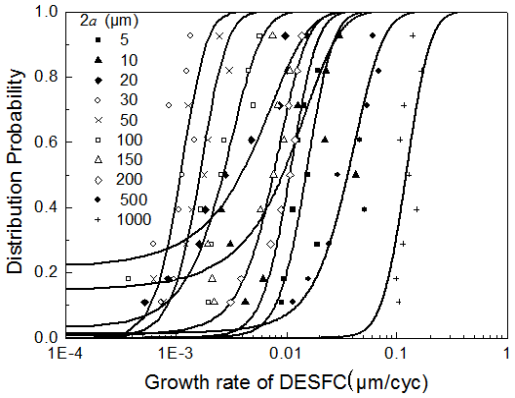

Fig. 6 Cumulative distribution curve of DESFC growth rate at given characteristic DESFC size

3.2. Analysis of DESFC growth rate at given characteristic fatigue life fraction

Average $(da/dN)_{m2}$, standard deviations $(da/dN)_{s2}$ and coefficients of variation Cv_2 of the 9 specimens at 10 given characteristic fatigue life fractions (f) are given in Table 5. The DESFC growth rates of all specimens and its mean value at characteristic f were given in Fig. 7. The mean value of the DESFC growth rate decreases with the increase of fatigue life fraction. The corresponding f at which the DESFC growth rate decreases is 0.1 and 0.5, respectively. Meanwhile, the evolution of $Cv_1$with the life frication f is given in Fig. 8, and which shows that coefficients of variation Cv_1 experienced two significant increases and then reached its maximum value at the life frication f = 0.1and f = 0.8. However, in the later period of PSC stage, the scatter declined gradually.

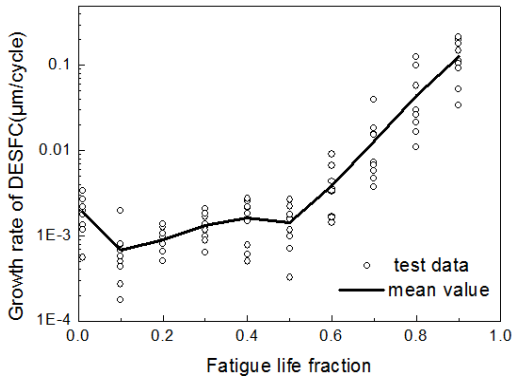

Fig. 7 DESFC growth rate at given fatigue life fraction

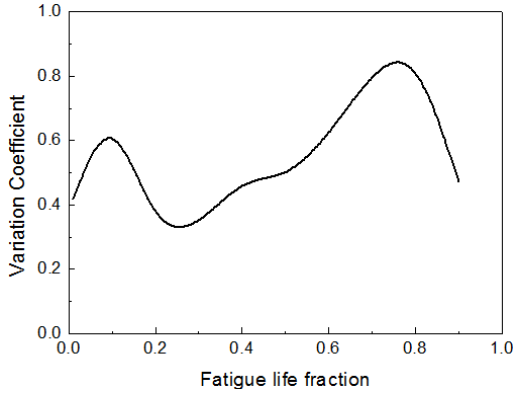

Fig. 8 Variation coefficient of DESFC growth rate at given fatigue life fraction

The linear correlation correlations of DESFC growth rates at 10 given characteristic life fraction f for 7 commonly used distributions mentioned above were listed in Table 6. From the view of best fit, the order of best fit is 3PWD, ND, ED, LND, 2PWD、EMVD2 and EMVD1. For the first six distributions, 10 groups of linear correlation coefficients were all greater than 0.85, but for EMVD1 it is relatively poor.

The prediction deviation, i.e., d_{F1} and d_{F2}, for 7 commonly used distributions of the right tail failure proportion for the DESFC growth rate data at given characteristic life frication f were given in Table 7. From which, conclusions can be drawn that ND is the best distribution for DESFC growth rates at given life frication f. For 10 groups of growth rate data, the prediction deviations for 9 groups of data show that $d_{F1} < 0$ and $d_{F1} < d_{F2}$ for 8 groups of data. It means that the predicted values are relatively conservative as long as the growth rate is greater than the value of $(d2a / dN)_n$. At the same time, the ND conforms to the consistency with the relevant fatigue physics of the increase of failure ratio with the increase of the growth rate [18]. In conclusion, ND is also the best distribution to describe the DESFC growth rates data at given fatigue life frication. Cumulative distribution curve of DESFC growth rate of each group were given in Fig. 9.

By Synthesizing Table 5 to Table 8 and Fig. 7 to Fig. 9, conclusions can be drawn as follows:

1. The mean curve of DESFC growth decreases twice with the increase of fatigue life fraction. The characteristic fatigue life fractions when these two growth rate decreases occur are 0.2 and 0.5, respectively. The standard deviations reach the minimum value as the life frication f is 0.2.

2. The scatter of DESFC growth rates data at given characteristic life frication f is large, and with the increase of f, the scatter of the DESFC growth rate data continue to fluctuate and decline in the later period of PSC stage.

3. ND is the best statistical distribution to describe the DESFC growth rates data at given characteristic fatigue life frication.

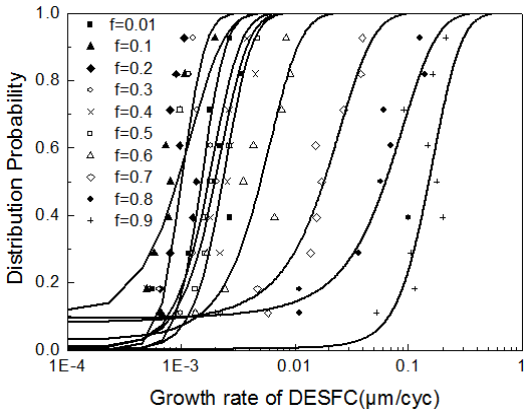

Fig. 9 Cumulative distribution curve of DESFC growth rate at given characteristic fatigue life fraction

Table 5

Statistical parameters of DESFC growth rate at given fatigue life fraction

f	$(da / dN)_{m2}$, $\times 10^{-6}$ m /cycle	$(d\,a /dN)_{s2}$, $\times 10^{-6}$ m/cycle	Cv_2
0.01	0.0020	0.0008	0.4173
0.1	0.0007	0.0005	0.7260
0.2	0.0009	0.0003	0.3056
0.3	0.0013	0.0004	0.3319
0.4	0.0016	0.0008	0.4851
0.5	0.0014	0.0007	0.4780
0.6	0.0039	0.0024	0.6138
0.7	0.0129	0.0106	0.8167
0.8	0.0443	0.0395	0.8914
0.9	0.1263	0.0596	0.4719

Table 6

Linear correlation correlations of DESFC growth rate at 10 given characteristic life fraction f for 7 commonly used distributions

f	R_{XY}						
	3PWD	2PWD	ND	LND	EMVD1	EMVD2	ED
0.01	0.9854	0.9854	0.9936	0.9534	0.9838	-0.9791	-0.9394
0.1	0.979	0.9659	0.866	0.9758	0.801	-0.9191	-0.947
0.2	0.9882	0.9785	0.9811	0.9882	0.9491	-0.9864	-0.9678
0.3	0.9975	0.9964	0.9945	0.9908	0.9722	-0.9908	-0.9624
0.4	0.9632	0.9628	0.9685	0.9425	0.9613	-0.9446	-0.8974
0.5	0.9884	0.9884	0.9954	0.9567	0.9785	-0.9879	-0.9551
0.6	0.9752	0.9465	0.931	0.9727	0.8691	-0.9713	-0.9874
0.7	0.99	0.9358	0.876	0.9718	0.8012	-0.9341	-0.9682
0.8	0.9737	0.9324	0.8959	0.9707	0.8214	-0.9476	-0.9771
0.9	0.9882	0.9882	0.9872	0.9614	0.9752	-0.9703	-0.9297

Table 7

Prediction deviation for 7 commonly used distributions of the right tail failure proportion for the DESFC growth rate data at given characteristic fatigue life fraction

DESFC	f	0.01	0.1	0.2	0.3	0.4	0.5	0.6	0.7	0.8	0.9
3PWD	d_{F1}	0.016	0.0029	0.0007	0.0014	-0.0131	0.0146	-0.0034	0.0014	-0.0383	0.0010
	d_{F2}	-0.0531	-0.0067	-0.0551	-0.0184	0.0347	-0.0253	-0.0154	-0.0225	0.0643	0.0291
2PWD	d_{F1}	0.016	-0.0221	-0.0241	-0.0055	-0.0294	0.0146	-0.0679	-0.0746	-0.0925	0.0010
	d_{F2}	-0.0531	0.0024	-0.0374	-0.0133	0.0398	-0.0253	0.003	-0.0152	0.0129	0.0291
ND	d_{F1}	0.0031	-0.1493	-0.0387	-0.0175	-0.0428	-0.0087	-0.131	-0.182	-0.1836	-0.0205
	d_{F2}	-0.0239	-0.0869	-0.0471	-0.0156	0.0395	-0.0004	-0.0469	-0.0975	-0.0776	0.0333
LND	d_{F1}	0.0403	0.0037	0.0011	0.0206	-0.0121	0.0389	-0.0516	-0.058	-0.0815	0.0244
	d_{F2}	-0.0804	0.0023	-0.0509	-0.0225	0.0449	-0.0445	0.0072	-0.0149	0.0236	0.0291
EMVD1	d_{F1}	-0.0225	-0.1493	-0.0592	-0.041	-0.0577	-0.0331	-0.1343	-0.1754	-0.1762	-0.0415
	d_{F2}	-0.017	-0.0757	-0.0385	-0.0131	0.0306	-0.0008	-0.0444	-0.0854	-0.0701	0.0251
EMVD2	d_{F1}	0.0426	-0.1304	0.0009	0.0234	-0.013	0.0321	-0.1104	-0.1747	-0.1793	0.0166
	d_{F2}	-0.0213	-0.0853	-0.0467	-0.0065	0.0616	0.0132	-0.035	-0.0986	-0.0734	0.0558
ED	d_{F1}	-0.3117	-0.1529	-0.6706	-0.5852	-0.2781	-0.2173	-0.2912	-0.1569	-0.1130	-0.2602
	d_{F2}	-0.4631	-0.1458	-0.6502	-0.5938	-0.2307	-0.3485	-0.2291	-0.0996	-0.0075	-0.2871

Table 8

Cumulative distribution parameters of ND for the DESFC growth rate data at given characteristic fatigue life fraction

f	Position parameter μ	Scale parameter σ
0.01	0.0129	0.006
0.1	0.0059	0.0091
0.2	0.0021	0.0049
0.3	0.0009	0.0004
0.4	0.0014	0.0007
0.5	0.0021	0.0016
0.6	0.0062	0.0039
0.7	0.0091	0.0043
0.8	0.0288	0.0195
0.9	0.1064	0.0421

4. Conclusions

The short fatigue crack replica tests of 9 hourglass shaped specimens were performed, and the DESFC growth rates were calculated based on obtained DESFC size and corresponding number of loading cycles. Meanwhile, three aspects, i.e., total fitting effect, consistency with the relevant fatigue physics, and safety of design evaluation were considered based on 10 groups of characteristic DESFC growth rate data according to given DESFC sizes and life fractions. Conclusions can be drawn as follows:

1. The DESFC growth rate and its mean value showed two significant decreases, which occurred when DESFC sizes were approximately equivalent to the average diameter of ferrites and the interval of the rich pearlite banded structures, respectively.

2. The scatter of the DESFC growth rate data is significant. It is fluctuant in the MSC stage because of the strong impact of the microstructures. However, in the PSC stage, it declines gradually with the further establishment of DESFC.

3. ND is the best statistical distribution to describe the DESFC growth rates data at either the given DESFC sizes or the given fatigue life fractions.

Acknowledgements

Present work is supported by the National Natural Science Foundation of China (51675446, 51275432 and U1534209), the National Key Research and Development Program of China (2016YFB1200403), and the Opening Project of State Key Laboratory of Traction Power (2015TPL_T13).

References

1. **Suresh, S.** 1999. Fatigue of Materials (translated by Wang ZG), Beijing: National Defense Industry Press,

452 p. (in Chinese).
2. **Zhao, Y.X.** 1998. Small crack behaviour and reliability analysis in low cycle fatigue, Chengdu: Southwest Jiaotong University, PH.D thesis, 162 p. (in Chinese).
3. **Miller, K.J.** 1987. The behaviour of short fatigue cracks and their initiation, Part Ⅰ-A review of two recent books, J. Fatigue Fract. Eng Mater Struct. 10: 75-91. http://dx.doi.org/10.1016/B978-0-08-034912-1.50183-1.
4. **Miller, K.J.** 1987. The behaviour of short fatigue cracks and their initiation, Part Ⅱ-A General Summary. J. Fatigue Fract. Eng Mater Struct. 10: 93-113. http://dx.doi.org/10.1016/B978-0-08-034912-1.50183-1.
5. **Pearson, S.** 1975. Initiation of fatigue cracks in commercial aluminium alloys and the subsequent propagation of very short cracks, Engineering Fracture Mechanics 7: 235-247. http://dx.doi.org/10.1016/0013-7944(75)90004-1.
6. **Ritchie, R.O.; Lankford, J.** 1986. Overview of small crack problem. In: small fatigue cracks A Publication of The Metallurgical Society, Warrendale, Pennsylvania, 1-5.
7. **Zhao, Y.X.; Wang, J.N.; Gao, Q.** 1999. Statistical evolution of small fatigue crack in 1Cr18Ni9Ti weld metal, Theor. Appl. Fract. Mech. 32: 55-64. http://dx.doi.org/10.1016/S0167-8442(99)00026-9.
8. **Goto, M.** 1991. Statistical investigation of the behaviour of microcracks in carbon steel, Fatigue Fract. Engng Mater. Struct. 14: 833-845. http://dx.doi.org/10.1111/j.1460-2695.1991.tb00715.x.
9. **Goto, M.** 1994. Statistical investigation of the behaviour of small cracks and fatigue life in carbon steel with different ferrite grain sizes, Fatigue Fract. Engng Mater. Struct. 17: 635-649. http://dx.doi.org/10.1111/j.1460-2695.1994.tb00262.x.
10. **Goto, M.** 1992. Scatter characteristics of fatigue life and the behaviour of small cracks, Fatigue Fract. Engng Mater. Struct. 15: 953-963. http://dx.doi.org/10.1111/j.1460-2695.1992.tb00024.x.
11. **Suh, C.M.; Lee, J.J.; Kang, Y.G.** 1990. Fatigue microcracks in type 304 stainless steel at elevated temperature, Fatigue Fract. Engng Mater. Struct. 13: 487-496. http://dx.doi.org/10.1111/j.1460-2695.1990.tb00619.x.
12. **Akiniwa, Y.; Tanaka, K.; Matsui, E.** 1988. Statistical characteristics of propagation of small fatigue cracks in smooth specimens of aluminium alloy 2024-T3, Material science and Engineering 104: 105-115. http://dx.doi.org/10.1016/0025-5416(88)90411-9.
13. **Zhao, Y.X.; Gao, Q.; Wang, J.N.** 2000. The evolution of short fatigue crack length and density: two approaches, Fatigue Fract Engng. Mater. 23: 929-941. http://dx.doi.org/10.1046/j.1460-2695.2000.00332.x.
14. **Zhao, Y.X.; Wang, J.N.; Gao, Q.** 2002. Density evolution of surface short fatigue crack propagation of 1Cr18Ni9Ti pipe-weld metal, J. Mater. Sci. Technol. 18: 266-270. http://dx.doi.org/10.3321/j.issn:1005-0302.2002.03.020.
15. **Yang, B.** 2010. Study on the random short fatigue crack behaviour of LZ50 axle steel, Chengdu: Southwest Jiaotong University, PH.D thesis. 162 p. (in Chinese).
16. **Zhao, Y.X.; Gao, Q.; Wang, J.N.** 1999. Interaction and evolution of short fatigue cracks, Fatigue & Fracture of Engineering Materials & Structures 22: 459-468. http://dx.doi.org/10.1046/j.1460-2695.1999.00195.x.
17. **Zhao, Y.X.; Sun, X.F.; Gao, Q.** 2001. Unified linear regression method for the analysis of seven commonly used statistical distributions, Journal of Mechanical Strength 23: 102-106 (in Chinese). http://dx.doi.org/10.3321/j.issn:1001-9669.2001.01.028.
18. **Zhao, Y.X.; Wang, J.N.; Gao, Q.** 2001. Unified approach for determining an appropriate assumed distribution of limited fatigue reliability data, China Mechanical Engineering 12: 1343-1347 (in Chinese). http://dx.doi.org/10.3321/j.issn:1004-132x.2001.12.005.

B. Yang, Z. Liao, B.Q. Ma, Y.Y. Wu, S.N. Xiao

STATISTICAL EVOLUTION OF SHORT FATIGUE CRACK GROWTH RATE FOR LZ50 AXLE STEEL

S u m m a r y

Initiation and propagation of short fatigue crack occupy most of the fatigue life of metal components with smooth surface. To characterize the statistical evolution behavior of short fatigue crack growth, totally 9 hourglass shaped specimens were fatigued under a loading frequency of 15 Hz by short fatigue crack replica test method. Afterwards, according to the "effective short fatigue crack criterion", replica test results were observed. Growth rate of DESFC for all specimens were obtained and analyzed. Combined with metallurgical test of LZ50 axle steel, conclusions can be drawn that it is the restraints of ferrite grain boundary and rich pearlite banded structure that cause the twice decline of DESFC growth rate. DESFC growth rates of each specimen at 10 given crack lengths and fatigue life fractions were obtained using linear interpolation method. The dispersion of DESFC growth rates was large and not steady in early cycles of MSC stage. But with the increase of loading cycles, the overall dispersion come down in later cycles of PSC stage gradually. Furthermore, seven commonly used distributions, i.e., 3PWD, 2PWD, ND, LND, EMVD1, EMVD2 and ED, were compared on three aspects, i.e., total fitting effect, consistency with the relevant fatigue physics, and safety of design evaluation. The results show that the ND, instead of 3PWD and 2PWD, is a good distribution for the growth rates of DESFC.

Keywords: short fatigue crack, growth rate, statistical evolution, LZ50 axle steel.

Received September 14, 2016
Accepted April 14, 2017